Goddard's **Li**DAR, **H**yperspectral & **T**hermal Imager **(G-LiHT)**

G-LiHT User Guide

Version 2.0

September 2021

Science Team

Principal Investigator: Bruce Cook
G-LiHT Scientist: Lawrence Corp
G-LiHT Co-Investigator: Douglas Morton

Material written by Bradford Wirt[1]

[1]KBR, Inc., contractor to the U.S. Geological Survey, Earth Resources Observation and Science (EROS) Center, Sioux Falls, South Dakota, USA. Work performed under USGS contract G0121D0001 for LP DAAC[2].

[2]LP DAAC Work performed under NASA contract NNG14HH33I.

Document History

Document Version	Publication Date	Description
1.0	March 2021	Original Documentation
2.0	September 2021	Updated for Recent Dataset Releases

Table of Contents

1 Dataset Overview 6

1.1 Background 6

2 Instruments and Specifications 6

2.1 Integrated PC 8

2.2 Scanning LiDAR 9

2.3 Profiling LiDAR 10

2.4 VNIR imaging spectrometer 11

2.5 VNIR irradiance spectrometer 12

2.6 Thermal imager 13

2.7 GPS-INS 14

2.8 G-LiHT Instrument and Specification Upgrades 15

3 Dataset Characteristics 16

3.1 G-LiHT LiDAR Point Cloud V001 16

3.2 G-LiHT Canopy Height Model KML V001 16

3.3 G-LiHT Canopy Height Model V001 17

3.4 G-LiHT Digital Terrain Model KML V001 17

3.5 G-LiHT Digital Terrain Model V001 18

3.6 G-LiHT Digital Surface Model V001 19

3.7 G-LiHT Trajectory Data V001 19

3.8 G-LiHT Aerial Orthomosaic V001 20

3.9 G-LiHT Flight Metadata V001 20

3.10 G-LiHT Hyperspectral Reflectance Mosaic V001 21

3.11 G-LiHT Hyperspectral Reflectance Swath V001 21

3.12 G-LiHT Hyperspectral Radiance Swath V001 22

3.13 G-LiHT Metrics V001 22

4 Frequently Asked Questions 23

5 Examples of Application 23

6 Dataset Access 23

7 Contact Information 24

8 Data Citation 24

9 Publications and References 24

List of Tables

Table 1 G-LiHT LiDAR Point Cloud V001 Collection Level Metadata 16

Table 2 G-LiHT LiDAR Point Cloud V001 Granule Level Metadata 16

Table 3 Canopy Height Model KML V001 Collection Level Metadata 16

Table 4 Canopy Height Model KML V001 Granule Level Metadata 17

Table 5 Canopy Height Model V001 Collection Level Metadata 17

Table 6 Canopy Height Model V001 Granule Level Metadata 17

Table 7 Digital Terrain Model KML V001 Collection Level Metadata 17

Table 8 Digital Terrain Model KML V001 Granule Level Metadata 18

Table 9 Digital Terrain Model V001 Collection Level Metadata 18

Table 10 Digital Terrain Model V001 Granule Level Metadata 18

Table 11 Digital Surface Model V001 Collection Level Metadata 19

Table 12 Digital Surface Model V001 Granule Level Metadata 19

Table 13 Trajectory V001 Collection Level Metadata 19

Table 14 Trajectory V001 Granule Level Metadata 20

Table 15 Aerial Orthomosaic V001 Collection Level Metadata 20

Table 16 Aerial Orthomosaic V001 Granule Level Metadata 20

Table 17 Flight Metadata V001 Collection Level Metadata 20

Table 18 Hyperspectral Reflectance Mosaic V001 Collection Level Metadata 21

Table 19 Hyperspectral Reflectance Mosaic V001 Granule Level Metadata 21

Table 20 Hyperspectral Reflectance Swath V001 Collection Level Metadata 21

Table 21 Hyperspectral Reflectance Swath V001 Granule Level Metadata 22

Table 22 Hyperspectral Radiance Swath V001 Collection Level Metadata 22

Table 23 Hyperspectral Radiance Swath V001 Granule Level Metadata 22

Table 24 Metrics V001 Collection Level Metadata 22

Table 25 Metrics V001 Granule Level Metadata 23

List of Figures

Figure 1 G-LiHT Flight Line Examples 7

Figure 2 G-LiHT System Specifications 7

Figure 3 G-LiHT Integrated PC Specifications 8

Figure 4 G-LiHT Scanning LiDAR Specifications 9

Figure 5 G-LiHT Profiling LiDAR Specifications 10

Figure 6 G-LiHT VNIR Imaging Spectrometer Specifications 11

Figure 7 G-LiHT Irradiance Spectrometer Specifications 12

Figure 8 G-LiHT Thermal Imager Specifications 13

Figure 9 G-LiHT GPS-INS Specifications 14

1 Dataset Overview

Goddard's LiDAR, Hyperspectral and Thermal Imager (G-LiHT) is a portable, airborne imaging system that simultaneously maps the composition, structure, and function of terrestrial ecosystems. G-LiHT's LiDAR instrumentation provides three-dimensional information about the distribution of foliage and canopy elements. Imaging spectroscopy discerns species composition and variations in biophysical variables. The thermal imager measures surface temperatures and detects heat and moisture stress.

G-LiHT enables data fusion studies by providing coincident data in time and space and provides fine-scale (<1 m) observations over areas that are needed in many ecosystem studies. The complementary nature of LiDAR, optical, and thermal data provides an analytical framework for the development of new algorithms for mapping plant species composition, plant function types, biodiversity, biomass and carbon stocks, and plant growth.

1.1 Background

With a need for more modern data products that can aid in the study and analysis of biodiversity and climate change, G-LiHT was designed to give scientists access to the data that is needed to understand the relationship between ecosystem form and function and stimulate the advancement of synergistic algorithms. The goal of G-LiHT's specific instrument integration effort is to test the use of new strategies for explicit description of ecosystem type and function, using diagnostic physiological remote sensing measurement in a variety of ways. These include (1) providing new insight into the photosynthetic functionality and productivity of a range of ecosystems under diverse environmental and climate conditions, (2) building upon existing abilities to monitor changes in vegetation function, composition and structure, quantifying the within-biome or ecosystem spatial and temporal variation for key parameters, and (3) generating a new strategy for monitoring key dynamic ecosystem processes to provide increased understanding about the effects of natural and human-induced changes.

G-LiHT has been used to collect hundreds of hours of data for NASA sponsored studies, including NASA's Carbon Monitoring System (CMS) and American Ice, Cloud, and land Elevation / Geoscience Laster Altimeter System (ICESat/GLAS) Assessment of Carbon (AMIGA-Carb). G-LiHT data is not intended to be a comprehensive dataset over a wide area. These acquisitions target a broad diversity of forest communities and ecoregions in North America, including the coterminous United States (CONUS), Alaska, Puerto Rico, and Mexico. Target sites are generally captured during times of vegetative growth and are frequently revisited over multiple years.

2 Instruments and Specifications

The G-LiHT system is comprised of commercial off the shelf components are aligned and rigidly mounted in a compact volume of $< 0.1\ m^3$ including centralized processing and data storage with a total system weight of 37 kg. Wire Rope Isolators (WR4-200-10, Endine Inc., Orchard Park, New York, USA) are used to mount the system to the aircraft and reduce the impact of aircraft vibrations. The system is weather resistant and can be mounted either internally to the aircraft over an appropriately sized view port or externally using a custom fabricated pod. Total power consumption is 220 W with a wide input voltage range from 9 to 36 V DC. Nominal flight altitude for G-LiHT is 335 m Above Ground Level (AGL) with a 60 degree Field of Vision (FOV) yielding a 387 m swath. The system includes internal processing and data storage capacity controlled via a remote desktop network connection and data are recorded to ejectable 500 Gb SSD media for efficient retrieval upon conclusion of the flight.

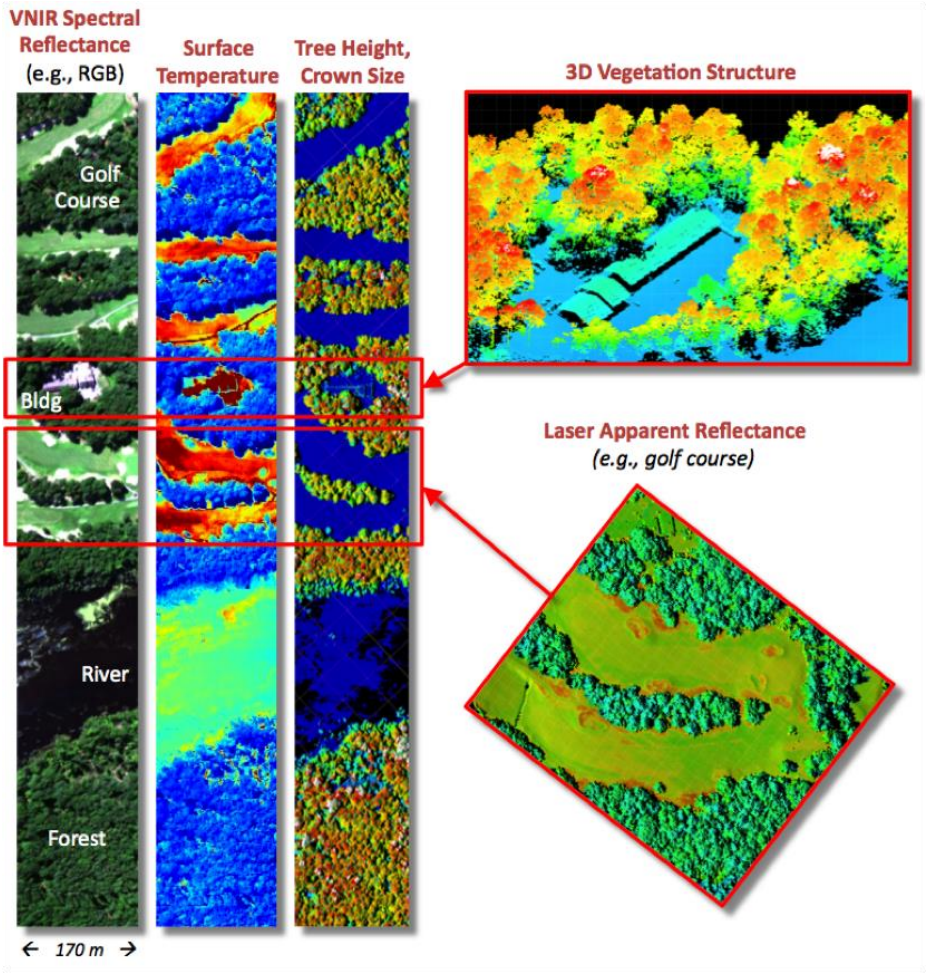

Figure 1. The complementary nature of LiDAR, optical and thermal data for characterizing the composition, structure, function, and stress of plant communities can be seen in a single G-LiHT flight line over contrasting cover types.

Operating Altitude	*335 m*
Ground Speed	*110 knots*
Field of View	*60°*
Swath	*387 m*
Power Consumption	*9-32 VDC, 210 W*
Operating temperature	*-10°C to 40°C*
Dimensions	*760x330x360 mm*
Weight	*82 lbs / 37 kg*

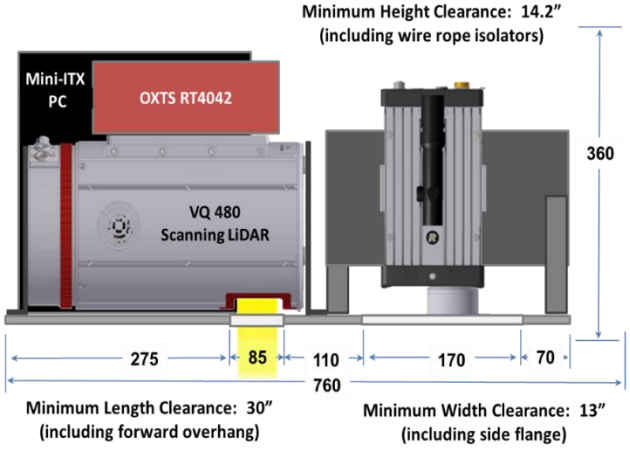

Figure 2. G-LiHT system specifications where minimum dimensions exclude movement during flight.

2.1 Integrated Personal Computer (PC)

G-LiHT's internal PC consists of the Jetway JC-111-B compact chassis with dual expansion slots and with a DC-DC wide input range M4-ATX power supply (Logic Supply, South Burlington, VT, USA). The PC uses a ZOTAC GF9300-I-E LGA 775 Mini ITX motherboard with the Intel Q9550S Yorkfield 2.83GHz 65W Quad-Core desktop processor and 8GB of PC2 6400 dual channel desktop memory. The PCIe expansion slot contains the PIXCI® EL1DB (EPIX, Buffalo Grove, IL, USA) dual base camera link frame grabber for 204 MB/s sustained data transfer of imaging spectrometer data. The motherboard Gigabit Ethernet, USB 2.0, and COM ports are relied on for simultaneous control and data transfer of all remaining G-LiHT components. Data are written to two 512 Gb SATA II solid state disks (one fixed mounted and one ejectable) with up to 180 MB/s sustained sequential write capability. User interfacing is accomplished via direct connection or using an Ethernet remote desktop connection to either a laptop or rack mount general purpose PC.

PC Form Factor	***Mini-ITX***
Processor	***I5 Quad Core***
Memory	***PC26400, 8Gb***
EPIX Frame Grabber	***EL1DB PCIe x4***
Power Supply	***M4-ATX, 250 W***
Operating System	***Win 7***
Operating temperature	***-40°C to 50°C***
Dimensions	***89 x63x34 mm***
Power consumption	***9 to 32 VDC, 105 W***

Figure 3. G-LiHT Integrated PC specifications.

2.2 Scanning LiDAR

The VQ-480 comprises an integrated high-performance laser rangefinder and a rotating polygon 3 facet mirror which deflects a 1550 nm Class 1 laser beam operating at a user selectable repletion rate up to 300 kHZ along a 60° swath perpendicular to the flight direction (fig. 4). The laser beam divergence is 0.3 milliradians (mrad) yielding a 10 cm beam diameter at the nominal operating altitude of 335 meters. The rotating multi-facet mirror scan speed is set to 100 scans/sec providing an angle measurement resolution of 0.001 degrees. For each laser shot the echo signal is digitized and the online waveform analysis provides highly accurate range results for multiple targets supplied via the integrated Gigabit Ethernet TCP/IP interface to G-LiHT's central computer. Each laser measurement is time tagged and accurately related to the single solution GPS/INS system via serial RS232 interface for a 1PPS TTL GPS-time input. The PC software RiACQUIRE provides a graphical user interface for scanner control and data acquisition with status feedback. RiACQUIRE is able to collect monitoring data from the laser scanner and online data provided by the IMU/GPS-system. Based on time-synchronized scan data, position, and attitude information, scan data coverage is calculated in real time to indicate appropriate point density at the target area.

The manufacturer's RiPROCESS software is used for managing, processing, analyzing, and visualizing data acquired with the airborne system. This project-oriented software enables the user to manage and process all acquired data within a single project. Main components of data management are project information, laser scanning system information (device information, mounting information, calibration data and laser configuration), navigation device information (position and orientation of the IMU and GNSS unit), original laser data, trajectory data and tie objects. Data processing tasks include, full waveform analysis and georeferencing laser data by merging laser data and position data derived from an INS/GNSS unit. These functions are provided by the manufacturer's applications RiANALYZE and RiWORLD respectively. As RiPROCESS is intended for mass data production in a multiple-workstation environment, these programs may be installed on different workstations. The multiple-workstation management is done by the program RiSERVER. RiPROCESS distributes the computational load by means of individual tasks to the available server-enabled processing tools optimizing data throughput. Data can be visualized in 2D and 3D in various ways, e.g. laser signal reflectivity, laser data density, color-encoded height visualization, and height differences within raster cells. Even huge amounts of data can be accessed fast for display in 3D. Quality of matching different data records can be assessed by visual inspection or by statistical analysis. RiPROCESS offers a tool to improve the calibration of the system, the relative fit of the scan data (to minimize inconsistencies between different laser datasets) and/or the absolute fit of the scan data in relation to a local/global coordinate system. This tool, named "scan data adjustment", allows the adjustment of several parameters such as the orientation and position offsets per laser data, per navigation device and of the Trajectory. In order to execute common tasks such as classification, triangulation and decimation by third-party software packages, RiPROCESS allows data export in the widely used LAS format.

Laser Wavelength	***1550 nm***
Repetition Rate	***up to 300 kHz***
Measurement Rate	***150,000 per s***
Beam Divergence	***0.3 mrad***
Accuracy	***25 mm***
Scan Speed	***100 per s***
Field of View	***600***
Laser Class	***1***
Power Consumption	***18 to 32 VDC, 65 W***
Operating temperature	***-10°C to 40°C***
Dimensions	***360 x 219 mm***
Weight	***28.7 lbs/13 kg***

Figure 4. Operating specifications for the VQ-480 Airborne Scanning LiDAR manufactured by Riegl, Riedenburgstrasse, Austria.

2.3 Profiling LiDAR

G-LiHT's profiling lidar, the LD321-A40 (Riegl USA, Orlando,FL), is a multi-purpose laser distance meter based upon precise time-of-flight laser range measurement. Real-time digital echo signal processing enables precise distance measurement for complex multi-target situations resolving up to 5 target distances per pulse. This portion of the system measures a transect parallel to the flight line accurately resolving the distance between the canopy top (minimum distance function) and ground elevation (maximum distance function) along with the vertical distribution of intercepted surfaces with an accuracy of ± 50 mm. The Class 1M laser diode emits at 905 nm with a beam divergence of 1.5 mrad after collimating optics to yield a 50 cm beam diameter at the nominal operating altitude of 335 meters. The LIDAR data yields a basic geometric representation of vegetation topography where structure can be resolved with reasonable accuracy. For each laser shot the echo signal is digitized and the online waveform analysis provides highly accurate range and amplitude results for up to 5 targets. Each laser measurement is time tagged and accurately related to a single solution GPS/INS system. Data transmission and system configuration are accomplished through a TCP/IP, 10/100 Mbit Ethernet connection to the central PC.

Laser Wavelength	***905 nm***
Repetition Rate	***10 kHz***
Measurement Rate	***up to 10 kHz***
Beam Divergence	***1.5 mrad***
Accuracy	***50 mm***
Laser Class	***1M***
Power	***12 to 28 VDC, 18 W***
Operating temperature	***-10°C to 50°C***
Dimensions	***248 x 130 x 112 mm***
Weight	***6.4 lbs/2.9 kg***

Figure 5. Operating specifications for the LD321-A40 laser distance meter manufactured by Riegl, Riedenburgstrasse, Austria.

2.4 VNIR Imaging Spectrometer

The major components of the hyperspectral imaging system are the Hyperspec™ VNIR Concentric Imaging Spectrometer (Headwall Photonics, Fitchburg, MA) and the ruggedized RA1000m/D digital fine gain imaging camera (Adimec, Stoneham, MA). The Hyperspec spectrometer enables high spectral and spatial resolution imaging through high efficiency f/2.0 telecentric optics and a high efficiency aberration-corrected convex holographic diffraction grating, providing an optical dispersion of 100 nm per mm over a 7.4 mm spatial by 6.0 mm spectral focal plane. The concentric spectrograph, based on the Offner design, enables imaging from 400-1000 nm over the full extent of an 18 mm tall 25 microns wide entrance slit. Hyperspec imaging spectrometer accepts a C-mount objective lens (Cinegon f/1.4 8mm, Schneider Optics, Hauppauge, NY) with high optical performance using ultra low dispersion glass and special broadband anti-reflection coating designed for enhanced visible to near-IR precision imaging. Coupled to the spectrometer is the RA1000m/D high speed rugged megapixel focal plane array allowing the acquisition of up to 75 progressive frames per second acquired through the PIXCI ECB1 PCI Express x4 base CameraLink interface. The camera uses a ½ inch interline 12 bit CCD imager in a 1004x1004 format with 7.4 micron pixels. Camera features include: a digital fine gain for adjustable camera sensitivity over a 60 dB dynamic range, electronic shuttering, and low smear characteristics. Furthermore, it offers ruggedized military specifications for severe operating environments. The camera is fully software controlled via a G-LiHT's internal PC with the serial communication channel of the CameraLink interface. Each image frame is coded with a PC timestamp synchronized with the common solution GPS/IMU system. Low altitude acquisitions and cross-calibration of a downwelling and upwelling spectrometers allows us to compute surface reflectance with minimal atmospheric effects.

Wavelength Range	***400-1000 nm***
Aperture	***F/2.0***
Dispersion per pixel	***0.72 nm***
Slit Width	***25 µm***
Slit Length	***18 mm***
Spectral Resolution	***5 – 6 nm***
Spectral Bands	***402***
Spatial Bands	***1004***
Dynamic Range	***68 db***
Frame Rate	***50 fps***
Weight	***6.7 lbs/3.0 kg***

Figure 6. Operating specifications for the HyperspecTM VNIR Concentric Imaging Spectrometer manufactured by Headwall Photonics, Fitchburg, MA. FOV = 2arctan(d/2f) = 49.64 deg, where f=8 mm lens and d=7.4 mm.

2.5 VNIR Irradiance Spectrometer

Downwelling radiance is measured by G-LiHT using the Ocean Optics USB 4000-VIS-NIR spectrometer (Dunedin, Fl, USA). Light energy is transmitted to the spectrometer through an upward looking opaline glass cosine diffuser with an 180° FOV. A 3 m, 100 µm single-strand optical fiber delivers the light energy through a 25 µm entrance slit and a multi-bandpass order-sorting filter. It then disperses via a fixed grating across a 3648-element Toshiba linear CCD array. The spectrometer covers the spectral range from 350 to 1100 nm with a native optical resolution to ~1.5 nm (FWHM). Power and communications occur through a USB 2.0 connection to the central PC. The downwelling radiometer is radiometrically cross-calibrated with the imaging spectrometer to enable atmospheric characterization and downwelling irradiance, and is used to provide enhanced surface reflectance product.

Array type	**Linear CCD**
Spectral band	**350 to 1000 nm**
# Pixels	**3648**
Pixel pitch	**8 x 200 µm**
SNR	**300:1**
Configured Data Rate	**1 Hz (16 bit)**
Operating temperature	**-40°C to 50°C**
Dimensions	**89 x63x34 mm**
Power consumption	**250mA @ 5VDC**

Figure 7. System specifications for the Ocean Optics USB 4000-VIS-NIR spectrometer (Dunedin, Fl, USA).

2.6 Thermal Imager

G-LiHT's thermal sensing capability originates from the Gobi-384 thermal imaging camera (Xenics, Leuven, Belgium). The broadband longwave infrared (LWIR) spectral range from 8 to 14 µm is covered by an uncooled a-Si microbolometer detector array (resistive amorphous silicon, FPA) with 384 cross track pixels and a 30° FOV. This compact component measuring 72 x 60 x 50 mm uses a Gigabit Ethernet TCP/IP interface to deliver 16-bit radiometrically calibrated thermal imaging data to G-LiHT's central computer running the Xenith software and graphical user interface. Each image frame is coded with a PC timestamp synchronized with the common solution GPS/IMU system.

Array type	***Microbolometer***
Spectral band	***8 µm to 14 µm***
# Pixels	***384 x 288***
Pixel pitch	***25 µm***
Sensitivity (NETD)	***≥ 50 mK @ 30°C***
Frame rate (full frame)	***25Hz (16 bit)***
Operating temperature	***-40°C to 50°C***
Focal length	***18 mm f/1***
Power consumption	***3.6 W @ 12V***

Figure 8. System specifications for the Gobi-384 LWIR thermal imaging camera manufactured by Xenics, Leuven, Belgium.

2.7 GPS-INS

The RT4041 (Oxford Technical Solutions, Oxfordshire, UK) is used as a single solution GPS/INS to obtain high precision position and attitude measurements. The six-axis inertial navigation system with three angular rate sensors (gyros) and three servo-grade accelerometers, incorporates an L1/L2 GPS receiver with an OmniStar HP decoder to deliver 0.1 m Circular Error Probably (CEP) positioning and 0.1° heading accuracies. Outputs from the system are derived from the measurements of the accelerometers and gyros using a 250Hz data rate. The real-time internal processing includes the strapdown algorithms (using a WGS-84 earth model), Kalman filtering, and in-flight alignment algorithms. The Kalman filter monitors the performance of the system and updates the measurements to maintain highly accurate measurements and correct its inertial sensor errors. The RT4041 is connected to a G3 Antenna with active L1 Glonass + GPS + OmniStar (Antcom P/N: G3Ant-42AT1, Torrance, CA, USA). For further GPS\INS antenna specifications review appendix A1.

GPS/INS data is stored on internal SD memory in a raw, unprocessed format (rd) which can be accessed via the TCP\IP data communications port. IMU lever arm and other offset coefficients are applied via the RT Post Process software by OXTS which converts the rd data to a proprietary binary format, referred to as NCOM and then exported to the ASCII (pos) format. During this step the inertial data is processed forwards and backwards in time and uses the best processing techniques available, including combining the results together in order to minimize the effects of GPS data drift. Where available the OmniStar HP satellite decoders is enabled giving 10 cm CEP in extended periods of open sky. Increased precision can be achieved where base station GPS data is available.

Update Rate	**250 Hz**
Position Acc.	**0.1 m**
Velocity Acc.	**0.07 km/hr**
Heading Acc.	**0.1 deg**
Acceleration Acc.	**0.01 m/s^2**
Angle Rate	**0.01 deg/s**
Power Consumption	**10-18 VDC, 20 W**
Operating temperature	**-10°C to 50°C**
Dimensions	**234x120x80 mm**
Weight	***4.85 lbs/2.2 kg***

Figure 9. Specifications for the OXTS RT4041 GPS/INS subsystem manufactured by Oxford Technical Solutions, Oxfordshire, UK.

2.8 G-LiHT Instrument and Specification Upgrades

The G-LiHT instruments and specifications have been upgraded from their initial design to better study the composition, structure, and function of terrestrial surfaces. New hardware includes the Riegl VQ 480i Dual Scanning LiDAR, Xenics Gobi-640 for thermal imaging, Phase One IXU-R 1000 for High Resolution Aerial Photos, and the Applanix POS AV V6 precision GPS. These instruments have been used on most G-LiHT flights and campaigns since 2017. More information on which instruments were used on a flight can be found in the G-LiHT metadata for each granule.

3 Dataset Characteristics

G-LiHT datasets are described below. Not all are currently active and will be added to the LP DAAC as they are made available.

3.1 G-LiHT LiDAR Point Cloud V001

Individual lidar return data, including 3D coordinates; classified ground returns, AGL heights, and lidar apparent reflectance, available in ASPRS LAS 1.1 format.

3.1.1 Collection Level

Table 1. Collection Level Metadata

Characteristic	Description
Collection	Community G-LiHT
Short Name	GLLIDARPC
DOI	10.5067/Community/GLIHT/GLLIDARPC.001
Temporal Resolution	Varies
Temporal Extent	2011-06-30 – Present
Spatial Extent	North America
Coordinate System	Universal Transverse Mercator (UTM)
Datum	WGS84
File Size	Varies by G-LiHT Flight
File Format	LAS (ASPRS LAS 1.1 format)

3.1.2 Granule Level

Table 2. Granule Level Metadata

Characteristic	Description
Number of Science Dataset (SDS) Layers	1
Columns/Rows	Variable
Pixel Size	~1 m

3.2 G-LiHT Canopy Height Model KML V001

Lidar-derived maximum canopy height and canopy rugosity available as a Google Earth overlay (KML).

3.2.1 Collection Level

Table 3. Collection Level Metadata

Characteristic	Description
Collection	Community G-LiHT
Short Name	GLCHMK
DOI	10.5067/Community/GLIHT/GLCHMK.001
Temporal Resolution	Varies
Temporal Extent	2011-06-30 – Present
Spatial Extent	North America
Coordinate System	Universal Transverse Mercator (UTM)
Datum	WGS84
File Size	Varies by G-LiHT Flight
File Format	KML

2.3.2 Granule Level

Table 4. Granule Level Metadata

Characteristic	Description
Number of Science Dataset (SDS) Layers	1
Columns/Rows	Variable
Pixel Size	~1 m

3.3 G-LiHT Canopy Height Model V001

Lidar-derived maximum canopy height and canopy rugosity as a raster data product (GeoTIFF).

3.3.1 Collection Level

Table 5. Collection Level Metadata

Characteristic	Description
Collection	Community G-LiHT
Short Name	GLCHMT
DOI	10.5067/Community/GLIHT/GLCHMT.001
Temporal Resolution	Varies
Temporal Extent	2011-06-30 – Present
Spatial Extent	North America
Coordinate System	Universal Transverse Mercator (UTM)
Datum	WGS84
File Size	~125 MB
File Format	GeoTIFF

3.3.2 Granule Level

Table 6. Granule Level Metadata

Characteristic	Description
Number of Science Dataset (SDS) Layers	1
Columns/Rows	Variable
Pixel Size	~1 m

3.4 G-LiHT Digital Terrain Model KML V001

Lidar-derived bare earth elevation aspect and slope available as a Google Earth overlay (KML).

3.4.1 Collection Level

Table 7. Collection Level Metadata

Characteristic	Description
Collection	Community G-LiHT
Short Name	GLDTMK
DOI	10.5067/Community/GLIHT/GLDTMK.001
Temporal Resolution	Varies
Temporal Extent	2011-06-30 – Present
Spatial Extent	North America
Coordinate System	Universal Transverse Mercator (UTM)
Datum	WGS84
File Size	Varies
File Format	KML

3.4.2 Granule Level

Table 8. Granule Level Metadata

Characteristic	Description
Number of Science Dataset (SDS) Layers	1
Columns/Rows	Variable
Pixel Size	~1 m

3.5 G-LiHT Digital Terrain Model V001

Lidar-derived bare earth elevation aspect and slope available as a raster data product (GeoTIFF).

3.5.1 Collection Level

Table 9. Collection Level Metadata

Characteristic	Description
Collection	Community G-LiHT
Short Name	GLDTMT
DOI	10.5067/Community/GLIHT/GLDTMT.001
Temporal Resolution	Varies
Temporal Extent	2011-06-30 – Present
Spatial Extent	North America
Coordinate System	Universal Transverse Mercator (UTM)
Datum	WGS84
File Size	Varies
File Format	GeoTIFF

3.5.2 Granule Level

Table 10. Granule Level Metadata

Characteristic	Description
Number of Science Dataset (SDS) Layers	1
Columns/Rows	Variable
Pixel Size	~1 m

3.6 G-LiHT Digital Surface Model V001

Lidar-derived bare earth elevation aspect, slope, and canopy rugosity available as a raster data product (GeoTIFF).

3.6.1 Collection Level

Table 11. Collection Level Metadata

Characteristic	Description
Collection	Community G-LiHT
Short Name	GLDSMT
DOI	10.5067/Community/GLIHT/GLDSMT.001
Temporal Resolution	Varies
Temporal Extent	2011-06-30 – Present
Spatial Extent	North America
Coordinate System	Universal Transverse Mercator (UTM)
Datum	WGS84
File Size	Varies
File Format	GeoTIFF

3.6.2 Granule Level

Table 12. Granule Level Metadata

Characteristic	Description
Number of Science Dataset (SDS) Layers	Varies (5 or 3)
Columns/Rows	Variable
Pixel Size	~1 m

3.7 G-LiHT Trajectory Data V001

Aircraft location and orientation (roll, pitch, yaw) available as a 3D Google Earth overlay (KML).

3.7.1 Collection Level

Table 13. Collection Level Metadata

Characteristic	Description
Collection	Community G-LiHT
Short Name	GLTRAJECTORY
DOI	10.5067/Community/GLIHT/GLTRAJECTORY.001
Temporal Resolution	Varies
Temporal Extent	2011-06-30 – Present
Spatial Extent	North America
Coordinate System	Universal Transverse Mercator (UTM)
Datum	WGS84
File Size	Varies
File Format	KML

3.8.2 Granule Level

Table 14. Granule Level Metadata

Characteristic	Description
Number of Science Dataset (SDS) Layers	1
Columns/Rows	Variable
Pixel Size	~1 m

3.8 G-LiHT Aerial Orthomosaic V001

High resolution orthorectified aerial photos that are stitched together with Agisoft Metashape photogrammetry.

3.8.1 Collection Level

Table 15. Collection Level Metadata

Characteristic	Description
Collection	Community G-LiHT
Short Name	GLORTHO
DOI	10.5067/Community/GLIHT/GLORTHO.001
Temporal Resolution	Varies
Temporal Extent	2011-06-30 – Present
Spatial Extent	North America
Coordinate System	Universal Transverse Mercator (UTM)
Datum	WGS84
File Size	<300 MB

File Format	GeoTIFF

3.8.2 Granule Level

Table 16. Granule Level Metadata

Characteristic	Description
Number of Science Dataset (SDS) Layers	4
Columns/Rows	N/A
Pixel Size	~1 in

3.9 G-LiHT Flight Metadata V001

Metadata for each flight available in PDF format.

3.9.1 Collection Level

Table 17. Collection Level Metadata

Characteristic	Description
Collection	Community G-LiHT
Short Name	GLMETA
DOI	10.5067/Community/GLIHT/GLMETA.001
Temporal Resolution	Varies
Temporal Extent	2011-06-30 – Present
Spatial Extent	North America
Coordinate System	N/A
Datum	N/A
File Size	<100 KB
File Format	PDF

3.10 G-LiHT Hyperspectral Reflectance Mosaic V001

At-sensor reflectance data computed at a nominal flying height of 335 meters.

3.10.1 Collection Level

Table 18. Collection Level Metadata

Characteristic	Description
Collection	Community G-LiHT
Short Name	GLREFM
DOI	10.5067/Community/GLIHT/GLREFM.001
Temporal Resolution	Varies
Temporal Extent	2011-06-30 – Present
Spatial Extent	North America
Coordinate System	Universal Transverse Mercator (UTM)
Datum	WGS84
File Size	~30 GB
File Format	HDR

3.10.2 Granule Level

Table 19. Granule Level Metadata

Characteristic	Description
Number of Science Data Set (SDS) Layers	114
Columns/Rows	Variable
Pixel Size	~1 in

3.11 G-LiHT Hyperspectral Reflectance Swath V001

At-sensor reflectance data computed at a nominal flying height of 335 meters, and available for individual swaths.

3.11.1 Collection Level

Table 20. Collection Level Metadata

Characteristic	Description
Collection	Community G-LiHT
Short Name	GLREFS
DOI	10.5067/Community/GLIHT/GLREFS.001
Temporal Resolution	Varies
Temporal Extent	2011-06-30 – Present
Spatial Extent	North America
Coordinate System	Universal Transverse Mercator (UTM)
Datum	WGS84
File Size	~30 GB
File Format	HDR

3.11.2 Granule Level

Table 21. Granule Level Metadata

Characteristic	Description
Number of Science Data Set (SDS) Layers	114
Columns/Rows	N/A
Pixel Size	~1 in

3.12 G-LiHT Hyperspectral Radiance Swath V001

Hyperspectral radiance data provided for individual swaths in radiometric units.

3.12.1 Collection Level

Table 22. Collection Level Metadata

Characteristic	Description
Collection	Community G-LiHT
Short Name	GLRADS
DOI	10.5067/Community/GLIHT/GLRADS.001
Temporal Resolution	Varies
Temporal Extent	2011-06-30 – Present
Spatial Extent	North America

Coordinate System	Universal Transverse Mercator (UTM)
Datum	WGS84
File Size	Varies
File Format	GeoTIFF

3.12.2 Granule Level

Table 23. Granule Level Metadata

Characteristic	Description
Number of Science Data Set (SDS) Layers	114
Columns/Rows	N/A
Pixel Size	~1 in

3.13 G-LiHT Metrics V001

Common lidar height and density metrics and return statistics available as raster data product (GeoTIFF).

3.13.1 Collection Level

Table 24. Collection Level Metadata

Characteristic	Description
Collection	Community G-LiHT
Short Name	GLMETRICS
DOI	10.5067/Community/GLIHT/GLMETRICS.001
Temporal Resolution	Varies
Temporal Extent	2011-06-30 – Present
Spatial Extent	North America
Coordinate System	Universal Transverse Mercator (UTM)
Datum	WGS84
File Size	Varies
File Format	GeoTIFF

3.13.2 Granule Level

Table 25. Granule Level Metadata

Characteristic	Description
Number of Science Data Set (SDS) Layers	1
Columns/Rows	Variable
Pixel Size	~13 m

4 Frequently Asked Questions (FAQs)

FAQs for G-LiHT data can be found on the LP DAAC website.

Additional questions include the following:

Why do some Digital Surface Model (DSM) granules contain only 3 science data layers while others contain 5?

Not all campaigns and flights included production of a Digital Surface Model (DSM) layer. Rugosity, Aspect, and Slope are derivatives of the Canopy Height Model (CHM) and Digital Terrain Model (DTM) layers. So, some flights may contain Rugosity, Aspect, and Slope, while others also include DSM and DSM Mean. When released, the GLMETA metadata dataset will provide detailed information on the configuration of the G-LiHT sensor for each flight.

5 Examples of Application

G-LiHT is a unique system that permits simultaneous measurements of vegetation structure, foliar spectra, and surface temperatures. The complementary nature lidar, optical, and thermal data provide an analytical framework for the development of new algorithms for mapping plant species composition, plant functional types, biodiversity, biomass and carbon stocks, and plant growth.

G-LiHT's instrument integration is optimized to test the use of new strategies for explicit description of ecosystem type and function, using diagnostic physiological remote sensing measurements to:

• Provide new insight into the photosynthetic functionality and productivity of a range of ecosystems under diverse environmental and climate conditions

• Build on our existing abilities to monitor changes in vegetation function, composition and structure to provide new spatially explicit remote sensing indicators of key dynamic biological processes

• Quantify the within-biome or ecosystem spatial and temporal variation for key parameters

• Generate a new strategy for monitoring key dynamic ecosystem processes and using this information as inputs to models to provide increased understanding about the effects of natural and human-induced changes on these ecosystems

6 Dataset Access

The following tools offer options to search the LP DAAC data holdings and provide access to the G-LiHT data:

Bulk download: LP DAAC Data Pool and DAAC2Disk
Search and Browse: NASA Earthdata Search

7 Contact Information

LP DAAC User Services
U.S. Geological Survey (USGS)
Earth Resources Observation and Science (EROS) Center
47914 252nd Street Sioux Falls, SD 57198-0001

Phone Number: 605-594-6116
Toll Free: 866-573-3222 (866-LPE-DAAC)
Fax: 605-594-6963
Email: LPDAAC@usgs.gov
Web: https://lpdaac.usgs.gov

To contact the Principal Investigator, please email Bruce Cook at bruce.cook@nasa.gov.

Project web site: G-LiHT

8 Data Citation

The recommended citation in APA or Chicago style is available on the Digital Object Identifier (DOI) Landing page .

An example of a citation using the Chicago style format for the GLCHMT dataset is provided below:

Cook, Bruce. *G-LiHT Canopy Height Model Mosaic V001*. 2021, distributed by NASA EOSDIS Land Processes DAAC, https://doi.org/10.5067/Community/GLIHT/GLCHMT.001. Accessed YYYY-MM-DD.

9 Publications and References

Cook, B. D., L. W. Corp, R. F. Nelson, E. M. Middleton, D. C. Morton, J. T. McCorkel, J. G. Masek, K. J. Ranson, V. Ly, and P. M. Montesano. 2013. NASA Goddard's Lidar, Hyperspectral and Thermal (G-LiHT) airborne imager. Remote Sensing 5:4045-4066, doi:10.3390/rs5084045.

Finley, A., S. Banerjee and B. D. Cook. Bayesian hierarchical models for spatially misaligned data in R. Methods in Ecology and Evolution (in review).

White, J. C., M. A. Wulder, A. Varhola, M. Vastaranta, N. C. Coops, B. D. Cook, D. Pitt, and M. Woods. 2013. A best practices guide for generating forest inventory attributes from airborne laser scanning data using the area-based approach. The Forestry Chronicle 89:722-723.

White, J.C., M. A. Wulder, A. Varhola, M. Vastaranta, N. C. Coops, B. D. Cook, D. Pitt, and M. Woods. 2013. A best practices guide for generating forest inventory attributes from airborne laser scanning data using the area-based approach. Information Report FI-X-10. Natural Resources Canada, Canadian Forest Service, Canadian Wood Fibre Centre, Pacific Forestry Centre, Victoria, BC. 50 p.

Neigh, C. S.R., J. G. Masek, P. Bourget, B. Cook, C. Huang, K. Rishmawi, and F. Zhao. Deciphering the precision of stereo IKONOS canopy height models for U.S. forests with G-LiHT airborne LiDAR. Remote Sensing (accepted).

Duncanson, L., B. Cook, G. J. Hurtt, and R. Dubayah. An efficient, multi-layered canopy delineation algorithm for mapping individual tree structure across multiple ecosystems. Remote Sensing of Environment (in press).

Duncanson, L., B. Cook, J. Rosette, J. Parker and R. Dubayah. Assessing the Utility of Individual crown information for Improving Biomass Density Estimation in the Western and Eastern USA. Remote Sensing of Environment (in review).

Babcock, C., J. Matney, A. O. Finley, A. Weiskittel, and B. D. Cook. 2013. Multivariate spatial regression models for predicting tree structure variables using LiDAR data. IEEE Journal of Selected Topics in Applied Earth Observations and Remote Sensing 6:6-14.

Dandois, J. P., and E. C. Ellis. 2013. High spatial resolution three-dimensional mapping of vegetation spectral dynamics using computer vision. Remote Sensing of Environment 136:259-276.

Sexton, J. O., X. -P. Song, M. Feng, P. Noojipady, A. Anand, C. Huang, D. -H. Kim, K. M. Collins, S. Channan, C. DiMiceli and J. R. Townshend. 2013. Global, 30-m resolution continuous fields of tree cover: Landsat-based rescaling of MODIS vegetation

continuous fields with lidar-based estimates of error. International Journal of Digital Earth 6:427-448, DOI: 10.1080/17538947.2013.786146

Finley, A. O., S. Banerjee, B. D. Cook, and J. B. Bradford. 2012. Hierarchical Bayesian spatial models for predicting multiple forest variables using waveform LiDAR, hyperspectral imagery, and large inventory datasets. International Journal of Applied Earth Observation and Geoinformation (in press). http://dx.doi.org/10.1016/j.jag.2012.04.007.

Corp, L.A., E.M. Middleton, P.K.E. Campbell, K.F. Huemmrich, Y.B. Cheng, C.S.T. Daughtry. 2010. Spectral indices to monitor nitrogen driven carbon uptake in field corn. Journal of Applied Remote Sensing. http://dx.doi.org/10.1117/1.3518455.

Cook, B. D., P. V. Bostad, E. Næsset, R. S. Anderson, S. Garrigues, J. Morisette, J. Nickeson, and K. J. Davis. 2009. Using LiDAR and Quickbird data to model plant production and quantify uncertainties associated with wetland detection and land cover generalizations. Remote Sensing of Environment 113:2366-2379. http://dx.doi.org/10.1016/j.rse.2009.06.017.

Rosette, J., J. Suárez, R. Nelson, S. Los, B. Cook, and P. North. 2012. Lidar remote sensing for biomass assessment. In L. Fatoyinbo (ed.) Remote Sensing of Biomass: Principles and Applications. InTech Open Access Publisher, http://www.intechweb.org, ISBN: 978-953-51-0313-4.

Babcock, C. R., A. Finley, and B. D. Cook. 2013. Modeling Forest Biomass and Productivity: Coupling Long-Term Inventory and G-LiHT Data. Abstract B41E-0451, 2013 Fall Meeting of the American Geophysical Union (AGU), San Francisco, CA, 9-13 Dec 2013.

Van Den Hoek, J., B. D. Cook, R. E. Kennedy, and J. Masek. 2013. Examining the Carbon Sequestration Potential of Regenerating Forests Using Pulse-Density Normalized High-Resolution Repeat LiDAR and Landsat Disturbance Data. Abstract B41F-03, 2013 Fall Meeting of the American Geophysical Union (AGU), San Francisco, CA, 9-13 Dec 2013.

Duncanson, L., B. D. Cook, O. Rourke, G. C. Hurtt, and R. Dubayah. 2013. Evaluating the Importance of Local Environment on Tree Structural Allometries. Abstract B43C-0513, 2013 Fall Meeting of the American Geophysical Union (AGU), San Francisco, CA, 9-13 Dec 2013.

Ranson, K., B. Cook, R. Nelson and G. Sun. 2013. Multisensor Airborne and Ground Studies of Siberian Arctic Forests. 2013 NASA Terrestrial Ecology Science Team Meeting, Scripps Seaside Forum, La Jolla, CA, 30 April - 2 May 2013.

Paynter, I., E. Saenz, X. Yang, Y. Liu, Z. Wang, C. Schaaf, Z. Li, A. Strahler, B. Cook, K. Krause, N. Leisso, C. Meier, D. Culvenor, G. Newnham, D. Jupp, J. Lovell, E. Douglas, J. Martel, S. Chakrabarti, T. Cook, G. Howe, K. Hewawasam, J. Thomas, J. Kim, S. Rouhani, Y. Yang, N. Pahlevan, Q. Sun, F. Peri, A. Erb. 2013. Lidar derived canopy height models of Harvard Forest. 24th Annual Harvard Forest Ecology Symposium, Fisher Museum, Harvard Forest, Petersham, MA, 19 March 2013.

Van Den Hoek, J., B. Cook, J. Masek, R. Kennedy and C. Tucker. 2013. Modeling aboveground biomass change using disparate lidar datasets in a managed northern Wisconsin forest. 4th North American Carbon Program (NACP) All-Investigators Meeting, Albuquerque, NM, 4-7 February 2013.

Duncanson, L., R. Dubayah, G. C. Hurtt, N. Pinto, B. D. Cook and A. Swatantran. 2012. How important is individual tree information for biomass modeling and mapping? Abstract B41E-0353, 2012 Fall Meeting of the American Geophysical Union (AGU), San Francisco, CA, 3-7 Dec 2012.

Montesano, P. M., R. Nelson, R. Dubayah, G. Sun and B. Cook. 2012. Uncertainty of remote measurements of biomass across a boreal forest gradient. Abstract B41E-0364, 2012 Fall Meeting of the American Geophysical Union (AGU), San Francisco, CA, 3-7 Dec 2012.

Cook, B., L. Corp, R. Nelson, D. Morton, K. J. Ranson, J. Masek, and E. Middleton. 2012. G-LiHT: Goddard's LiDAR, Hyperspectral and Thermal Airborne Imager. Silvilaser, Vancouver, Canada, 16-19 September 2012.

Duncanson, L., R. Dubayah, M. Brolly, B. Cook, and A. Swatantran. 2012. A novel canopy delineation algorithm for discrimination of understory and overlapping crowns with high-resolution LiDAR. Silvilaser, Vancouver, Canada, 16-19 September 2012.

Rosette, J., B. Cook, R. Nelson, C. Huang, J. Masek, C. Tucker, G. Sun, W. Huang, P. Montesano, J. Rubio-Gil, J. Ranson. 2012. Biomass change estimation within NASA's Carbon Monitoring System. Silvilaser, Vancouver, Canada, 16-19 September 2012.

North, P., J. Rosette, D. Harding, B. Cook, P. Dabney, S. Valett, J. Parker, J. Brinks. 2012. Simulation of micro-pulse photon counting lidar using the FLIGHT radiative transfer model for SIMPL and ICESat-2. Silvilaser, Vancouver, Canada, 16-19 September 2012.

Suárez, J., J. Rosette, R. Nelson, N. Pinto, R. Dubayah, B. Cook and T. Fatoyinbo. 2012. The Carbon Monitoring System: preliminary results of biomass inventory using small footprint LiDAR from archive. Silvilaser, Vancouver, Canada, 16-19 September 2012.

Dubayah, R., J. Suárez, R. Nelson, J. Rosette, A. Swatantran, N. Pinto, R. Birdsey, K. Johnson, B. Cook, A. Armstrong, C. Huang, L. Duncanson, and G. Hurtt. 2012. High-Resolution Carbon Estimation in NASA's Carbon Monitoring System. ForestSAT 2012, 11-14 September 2012, Oregon State University, Corvallis, OR.

Duncanson, L., R. Dubayah, C. Huang, K. Dolan, N. Pinto, J. Fisk, B. Cook and G. Hurtt. 2012. Modeling tree size distribution as a function of stand age: an application of novel remote sensing datasets. ForestSAT 2012, 11-14 September 2012, Oregon State University, Corvallis, OR.

Rosette, J., B. Cook, R. Nelson, L. Corp, C. Field, J. Masek, D. Morton, B. Middleton, J. Ranson, P. Decola, and J. Degnan. 2012. Multi-sensor, high resolution remote sensing for forest assessment within NASA's Carbon Monitoring System initiative (CMS). ForestSAT 2012, 11-14 September 2012, Oregon State University, Corvallis, OR.

Cook, B. D., L. A. Corp, H. A. Margolis, J. Masek, E. M. Middleton, P. Montesano, D. Morton, R. Nelson, K. J. Ranson, J. Rosette, G. Sun, K. J. Thome. 2011. G-LiHT: Goddard's LiDAR, Hyperspectral, and Thermal airborne imager. NASA Carbon Cycle and Ecosystem Joint Science Workshop, Alexandria, VA, 3-7 October 2011.

Pinto, N., R. Dubayah, M. Simard, S. Saatchi, B. Cook and P. Siqueira. 2011. Scaling up forest allometry with lidar and radar remote sensing. ESA Annual Meeting, Austin, Texas, 7-12 August 2011.

Cook, B. D., R. Nelson, B. Middleton, L. Corp, D. Morton, J. Masek and J. Ranson. 2011. G-LiHT: Goddard's LiDAR, Hyperspectral and Thermal Airborne Imager. 2011 HyspIRI Science Symposium on Ecosystem Data Products, Greenbelt, MD, 17-18 May 2011.

Corp, L.A., B.D. Cook, E.M. Middleton, Y.B. Cheng, K.F. Huemmrich, and P.K.E. Campbell, P.K.E (2010b). FUSION: A fully ultraportable system for imaging objects in nature, Proceedings, International Geosci. Rem. Sens. Symp. (IGARSS), 25-30 July 2010, Honolulu, HI.